Accepted Manuscript

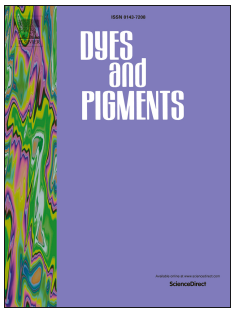

The impact of adjusting auxiliary donors on the performance of dye-sensitized solar cells based on phenothiazine D-D-π-A sensitizers

Shu-Guang Chen, Hai-Lang Jia, Xue-Hai Ju, He-Gen Zheng

PII: S0143-7208(17)31228-7

DOI: 10.1016/j.dyepig.2017.06.068

Reference: DYPI 6089

To appear in: *Dyes and Pigments*

Received Date: 27 May 2017

Revised Date: 28 June 2017

Accepted Date: 28 June 2017

Please cite this article as: Chen S-G, Jia H-L, Ju X-H, Zheng H-G, The impact of adjusting auxiliary donors on the performance of dye-sensitized solar cells based on phenothiazine D-D-π-A sensitizers, *Dyes and Pigments* (2017), doi: 10.1016/j.dyepig.2017.06.068.

Graphical Abstract

The Impact of Adjusting Auxiliary Donors on the Performance of Dye-sensitized Solar Cells Based on Phenothiazine D-D-π-A Sensitizers

Shu-Guang Chen, Hai-Lang Jia, Xue-hai Ju and He-Gen Zheng*

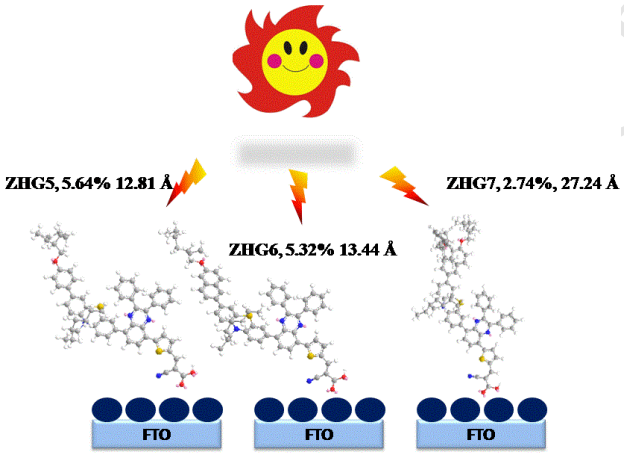

Auxiliary donor with overlarge steric hindrance will have smaller tilt angle of dye anchored on TiO_2 and will lead to more dye loading amount but serious intermolecular π-π aggregation effects.

The Impact of Adjusting Auxiliary Donors on the Performance of Dye-sensitized Solar Cells Based on Phenothiazine D-D-π-A Sensitizers

Shu-Guang Chen [a], Hai-Lang Jia [a], Xue-hai Ju [b] and He-Gen Zheng [a,*]

[a]*State Key Laboratory of Coordination Chemistry, School of Chemistry and Chemical Engineering, Collaborative Innovation Center of Advanced Microstructures, Nanjing University, Nanjing 210093, P. R. China. E-mail: zhenghg@nju.edu.cn; Fax: +86-25-89682309*

[b]*School of Chemical Engineering, Nanjing University of Science and Technology, Nanjing 210094, P. R. China. E-mail: xhju@mail.njust.edu.cn*

Received Oct XX, 2015

ABSTRACT

Three new D-D-π-A Sensitizers **ZHG5**, **ZHG6** and **ZHG7** have been prepared by gradually improving the steric hindrance of auxiliary donors and the power conversion efficiencies (PCE) are 5.64%, 5.32% and 2.74%. UV-Vis absorption indicates that the molar extinction coefficients decrease with the increased steric hindrance of auxiliary donors. X-ray photoelectron spectroscopy (XPS) indicates that the tilt angles of **ZHG5** and **ZHG6** anchored on the TiO_2 film are similar and **ZHG7** is almost standing rather vertical on the TiO_2 film with the smallest tilt angle. The results of dye desorption and XPS experiments indicate that the dye loading amount of **ZHG6** with larger steric hindrance is lower than that of **ZHG5**, **ZHG7** with largest auxiliary donor has the

maximum loading amount probably due to its smallest tilt angle. Larger auxiliary donor of **ZHG6** leads to higher open circuit voltage (V_{oc} = 734 mV) but lower shorter circuit current (J_{sc} = 12.63 mA cm^{-2}) compared with that of **ZHG5** (V_{oc} = 730 mV, J_{sc} = 12.06 mA cm^{-2}). However, dense packing of dye **ZHG7** anchored on the TiO_2 leads to more serious intermolecular π-π aggregation effects. Perhaps this effect and lowest molar extinction coefficient are the reason that DSSC based on **ZHG7** have the lowest PCE. So above results indicate that auxiliary donor with overlarge steric hindrance will have smaller tilt angle of dye anchored on TiO_2 and may lead to more dye loading amount but serious intermolecular π-π aggregation effects.

Keywords: Auxiliary donors; D-D-π-A sensitizers; Dye-sensitized solar cells; Photovoltaic property.

*Corresponding author.

E-mail address: zhenghg@nju.edu.cn (H.-G. Zheng)

1. Introduction

As result of the growing energy demand and the pollution of fossil fuels, people urgently need new energy to replace fossil energy. Dye-sensitized solar cells (DSSCs) as a new generation of photovoltaic technology provide a direction to develop new energy, so during the last twenty years DSSCs have got tremendous attention since 1991[1]. The highest photoelectric conversion efficiencies (PCE) of DSSCs based on ruthenium-complexes and Zn-porphyrins are 11.9% and 13%, respectively [2]. Although these two kinds of sensitizers have made considerable progress, metal-free organic dyes are attracting more and more attention in recent years because of their variable structures,

simple synthesis and high molar extinction coefficients [3]. The highest PCE (14%) of DSSC based on pure organic dyes is reported by Minoru Hanaya and co-workers [4]. So the metal-free dyes have provided more options to improve the performances of DSSCs. However the rapid recombination reaction between the mesoporous TiO_2 surface and electrolyte becomes the one of key limiting factors of improving the DSSCs performance. So how to suppress this kind of electron recombination effect becomes the one of main research directions. The Hagfeldt and co-workers have reported the dye D35 with *o,p*-dibutoxyphenyl as electron donor and got encouraging results [5]. Since then, numbers of dyes with bulky donors have been designed to improve the performance of DSSCs. For example, Tian and co-workers have reported dye Y422 with bulky indoline-based donor and effectively improved the PCE of DSSCs and reached 10.65% [6]. These excellent works indicate that suppressing the recombination reaction with steric effect to improve the DSSCs performance is an effective method. In general, the steric hindrance is expanded mainly by introduction of long side chains or increased conjugation or both [7]. But there are few samples to further improve the steric hindrance of sensitizers by introducing propeller auxiliary donor.

XPS can provide the information about the molecular structure, valence state, element composition and chemical bond. The photon beam of XPS only can produce little damage to the samples. So XPS is a powerful and suitable tool for investigating the adsorption properties of dyes anchored on TiO_2 to reveal the possible reasons of different device performances. But there are only several documents about investigating the cells performance of dyes with different side alky chain by using XPS, so the samples about investigating the adsorption properties of dyes with different auxiliary donors on the TiO_2

film with XPS are fewer.

Based on the above considerations we have synthesized three new D-D-π-A dyes (**ZHG5**, **ZHG6** and **ZHG7**) based on phenothiazine by adjusting the auxiliary donor as shown in Fig 1. The dye **ZHG5** has been prepared with alkoxy phenyl as the auxiliary donor. The alkoxy naphthalene has been employed to replace the cyclobenzene to improve the conjugation of auxiliary donor in dye **ZHG6**. In order to further improve the steric hindrance of auxiliary donor, we have introduced the alkoxy dinaphthalene into the dye **ZHG7** because of its propeller type structure. 2,3-Diphenylquinoxaline has been chosen as the assistant electron-withdrawing unit in three dyes because it can facilitate the intramolecular charge transfer (ICT) and improve the light-harvesting ability [8]. Thiophene is usually thought to have better conjugacy, so it has been introduced into all the dyes as part of linkers [9]. Cyanoacrylic acid as a kind of effective acceptor has been chosen as anchor group in three dyes [10]. The different device performances of DSSCs based on above sensitizers are investigated by electrochemical, photophysical, and photovoltaic characterizations in combination with theoretical calculations. XPS has been used to get insight to the adsorption properties and reveals the possible reasons of different device performances caused by tuning the auxiliary donors.

2. Experiment section

2.1. Materials and measurements

All solvents and reagents were purchased from commercial suppliers and used as received unless otherwise specified. *N*, *N*-Dimethylformamide were dried and distilled from CaH_2, toluene and tetrahydrofuran were dried and distilled from Na.

The ^{1}HNMR and ^{13}CNMR spectra were recorded on a Bruker DRX (300/400 MHz) NMR spectrometer. The mass spectra were measured in EI Mass Spectrometer (LCQ Fleet).

2.2. Fabrication of DSSCs

We cleaned the FTO glass plates (15 Ω per square) with detergent solution in ultrasonic bath for 0.5h two times before preparing the TiO_2 film by screen printing and then washed by water and ethanol. The FTO glass plates were then treated with 40 mM $TiCl_4$ (aqueous) at 70^{o}C for 30 min and washed with water and ethanol. The TiO_2 films were prepared by sintered gradually up to 500°C and kept at this temperature before cooling. The TiO_2 films were immersed in 40mM $TiCl_4$ at 70^{o}C for 30 min again and washed with water and ethanol. Finally the films were sintered at 500^{o}C for 30min. After cooling to 25^{o}C, the films were immersed into 0.3 mM ZHG dyes solution in THF/ethanol (1:1) for 18 h at room temperature to complete the loading of sensitizers. The photoanodes were sealed with platinum counter electrodes by a hot-melt film (25-μm-thick Surlyn, Dupont). The electrolytes were introduced to the cells via one predrilled hole back in the counter electrodes and thin glass covers by heating with electric soldering iron. The I^{-}/I_3^{-} electrolyte consisted of 0.6 M 1-butyl-3-methylimidazolium iodide (BMII), 30 mM I_2, 50 mM LiI, 0.5 M tert-butylpyridine and 0.1 M guanidiniumthiocyanate (GuNCS) in a mixed acetonitrile and valeronitrile (85:15, V/V) solvent.

2.3. Synthesis and characterization

*2.3.1. Synthesis of 2-(4-((2-ethylhexyl)oxy)phenyl)-4,4,5,5-tetramethyl-1,3,2-dioxaborolane (**2a**)*

A mixture of compound **1a** (10 g, 35.21 mmol), bis(pinacolato)diboron (9.8 g, 38.73 mmol), Pd(dppf)Cl_2 (1.28 g, 1.76 mmol) and AcOK (10 g, 105.63 mmol) in 200 ml 1,4-dioxane was heated at 100^{o}C overnight under N_2. The reaction solution was removed under vacuum and water was added. The water phase was then extracted with DCM. Combined organic phase was dried by Na_2SO_4. Column chromatography over silica gel with petroleum ether/DCM (4/1) gives out target compound **2a** as colourless oil liquid (6.39 g, 55%). ^{1}H NMR (300 MHz, $CDCl_3$) δ 7.74 (d, J = 8.7 Hz, 2H), 6.89 (d, J = 8.7 Hz, 2H), 3.86 (d, J = 5.9 Hz, 2H), 1.72 (dd, J = 6.1, 6.0 Hz, 1H), 1.53 - 1.36 (m, 4H), 1.33 (s, 16H), 0.96 - 0.87 (m, 6H). ^{13}C NMR (101 MHz, $CDCl_3$) δ 162.08, 136.52, 134.80, 131.28, 127.72, 113.93, 83.48, 70.26, 39.39, 30.57, 29.12, 24.89, 23.91, 23.09, 14.13, 11.15. HRMS (EI+): [M+H$^+$] Calcd for $C_{20}H_{33}BO_3$, 333.2596; found, 333.2595.

*2.3.2. Synthesis of 3-bromo-7-(4-((2-ethylhexyl)oxy)phenyl)-10-octyl-10H-phenothiazine (**4a**)*

A mixture of compound **2a** (6.42 g, 19.94 mmol), 3 (9.35 g, 19.94 mmol), Pd(PPh_3)$_4$ (1.0 g, 0.997 mmol) and K_2CO_3 (8.3 g, 59.82 mmol) in 165 ml 1,4-dioxane/H_2O was heated at 100^{o}C overnight under N_2. The reaction solution was removed under vacuum and water was added. The water phase was then extracted with DCM. Combined organic phase was dried by Na_2SO_4. Column chromatography over silica gel with petroleum ether/DCM (20/1) gives out target compound **4a** as light yellow oil liquid (5.83 g, 49%). ^{1}H NMR (400 MHz, $CDCl_3$) δ 7.43 (d, J = 8.6 Hz, 2H), 7.32 (d, J = 7.8 Hz, 2H), 7.28 - 7.20 (m, 2H), 6.94 (d, J = 8.6 Hz, 2H), 6.89 (d, J = 7.9 Hz, 1H), 6.71 (d, J = 8.5 Hz, 1H), 3.86 (d, J = 5.6 Hz, 2H), 3.69 (s, 2H), 1.95 - 1.89 (m, 1H), 1.77 - 1.69 (m, 1H), 1.49 - 1.45 (m, 4H), 1.33 - 1.25 (m, 12H), 0.95 - 0.84 (m, 12H). ^{13}C NMR (101 MHz, $CDCl_3$) δ 158.87, 144.95, 144.05, 135.69, 132.22, 129.85, 127.82, 127.52, 125.63, 125.38, 116.96, 116.15, 114.88, 114.40, 70.62, 51.16, 39.46, 35.88, 30.75, 30.61, 29.16, 28.63, 24.05, 23.95, 23.14, 23.13, 14.18, 14.10, 11.20, 10.55. HRMS (EI+): [M+H$^+$] Calcd for $C_{34}H_{44}BrNOS$, 594.2400; found, 594.2386.

*2.3.3. Synthesis of 3-(4-((2-ethylhexyl)oxy)phenyl)-10-octyl-7-(4,4,5,5-tetramethyl-1,3,2-dioxaborolan-2-yl)-10H-phenothiazine (**6a**)*

A mixture of compound **4a** (4.86 g, 8.14 mmol), bis(pinacolato)diboron (2.17 g, 8.54 mmol), $Pd(dppf)Cl_2$ (0.3 g, 0.41 mmol) and AcOK (2.4 g, 24.12 mmol) in 100 ml 1,4-dioxane was heated at 100°C overnight under N_2. The reaction solution was removed under vacuum and water was added. The water phase was then extracted with DCM. Combined organic phase was dried by Na_2SO_4. Column chromatography over silica gel with petroleum ether/DCM (4/1) gives out target compound **6a** as light yellow oil liquid (4.3 g, 86%). ^{1}H NMR (400 MHz, $CDCl_3$) δ 7.58 (dd, J = 6.8, 1.4 Hz, 2H), 7.44 (d, J = 8.7 Hz, 2H), 7.33 - 7.28 (m, 2H), 6.96 - 6.91 (m, 2H), 6.88 - 6.85 (m, 2H), 3.86 (dd, J = 5.8, 1.0 Hz, 2H), 3.76 (d, J = 7.0 Hz, 2H), 1.98 - 1.89 (m, 1H), 1.79 - 1.68 (m, 1H), 1.40 - 1.25 (m, 28H), 0.96 - 0.81 (m, 12H). ^{13}C NMR (101 MHz, $CDCl_3$) δ 158.77, 148.36, 143.93, 135.51, 134.04, 132.36, 128.75, 127.49, 125.54, 125.23, 116.08, 115.17, 114.80, 83.68, 70.59, 39.42, 35.92, 30.74, 30.56, 29.72, 29.11, 28.62, 24.86, 24.02, 23.90, 23.08, 14.12, 14.04, 11.14, 10.50. HRMS (EI+): [M+H$^+$] Calcd for $C_{40}H_{56}BNO_3S$, 642.4147; found, 642.4138.

*2.3.4.3-(8-bromo-2,3-diphenylquinoxalin-5-yl)-10-octyl-7-(4-(octyloxy)phenyl)-10H-phenothiazine (**8a**)*

A mixture of compound **6a** (2.92 g, 4.56 mmol), 7 (2.0 g, 4.56mmol), $Pd(PPh_3)_4$ (0.53 g, 0.456 mmol) and K_2CO_3 (1.90 g, 13.68 mmol) in 110 ml 1,4-dioxane/H_2O was heated at 100°C overnight under N_2. The reaction solution was removed under vacuum and water was added. The water phase was then extracted with DCM. Combined organic phase was dried by Na_2SO_4. Column chromatography over silica gel with petroleum ether/DCM (10/1) gives out target compound **8a** as red soild. (2.8 g, 70%).^{1}H NMR (400 MHz, $CDCl_3$) δ 8.08 (d, *J* = 7.8 Hz, 1H), 7.91 (br, 2H), 7.71 (dd, *J* = 7.8, 1.5 Hz, 2H), 7.65 (dd, *J* = 5.2, 3.2 Hz, 4H), 7.61 - 7.54 (m, 2H), 7.41-7.34 (m, *J* = 7.8, 6.3 Hz, 9H), 6.95 (d, *J* = 8.4 Hz, 2H), 3.88 (d, *J* = 4.9 Hz, 4H), 2.03-2.00 (m, 1H), 1.76-1.71 (m, 1H), 1.58 - 1.37 (m, 16H), 1.03 - 0.73 (m, 12H). ^{13}C NMR (101 MHz, $CDCl_3$) δ 158.82, 154.13, 152.78, 152.39, 139.36, 139.13, 138.98, 138.69, 138.57, 138.53, 137.99, 133.12, 133.05, 130.30, 130.27, 130.20, 129.91, 129.61, 129.33, 129.17, 128.40, 128.26, 127.54,

125.63, 125.43, 124.55, 124.08, 123.76, 122.61, 116.13, 115.26, 114.87, 70.64, 39.47, 31.53, 30.86, 30.62, 30.29, 29.17, 28.73, 24.16, 23.96, 23.18, 23.15, 14.21, 14.16, 11.23, 10.65. HRMS (EI+): [M+H$^+$] Calcd for $C_{54}H_{56}BrN_3OS$, 874.3400; found, 874.3398.

*2.3.5. Synthesis of the dye **ZHG5***

A mixture of compound **8a** (2.8 g, 3.2 mmol), 9 (1.0 g, 6.4 mmol), $Pd(PPh_3)_4$ (0.4 g, 0.32 mmol) and K_2CO_3 (1.4 g, 9.6 mmol) in 110 ml 1,4-dioxane/H_2O was heated at 100^{o}C overnight under N_2. The reaction solution was removed under vacuum and water was added. The water phase was then extracted with DCM. Combined organic phase was dried by Na_2SO_4. Column chromatography over silica gel with petroleum ether/DCM (2/1) gives out 1.0 g target compound **10a** as red soild and the yield is 34%. A mixture of compound **10a** (1 g, 1.1 mmol), cyanoacetic acid (1.9 g, 22 mmol) and NH_4OAc (2.5 g, 33 mmol) in 30 ml CH_3COOH solution was heated at 120^{o}C overnight under N_2. The reaction solution was removed under vacuum and water was added. The water phase was then extracted with DCM. Combined organic phase was dried by Na_2SO_4. Column chromatography over silica gel with petroleum ether/DCM (1/1) gave out 0.23 g **ZHG5** dye as dark red solid and the yield is 22%. ^{1}H NMR (400 MHz, DMSO) δ 8.53 (d, J = 8.0 Hz, 1H), 8.25 (s, 1H), 8.13 (d, J = 3.8 Hz, 1H), 8.02 (d, J = 7.9 Hz, 1H), 7.87 - 7.79 (m, 4H), 7.76 (d, J = 8.2 Hz, 1H), 7.58 (dd, J = 7.3, 5.6 Hz, 4H), 7.47 (d, J = 6.6 Hz, 2H), 7.45 - 7.41 (m, 3H), 7.39 - 7.33 (m, 3H), 7.22 (d, J = 8.6 Hz, 1H), 7.14 (d, J = 9.2 Hz, 1H), 7.00 (d, J = 8.7 Hz, 2H), 3.89 (d, J = 5.6 Hz, 4H), 2.04 – 1.88 (m, 3H), 1.77 - 1.63 (m, 1H), 1.46 - 1.29 (m, 14H), 0.91 - 0.82 (m, 12H). ^{13}C NMR (101 MHz, *D8*-THF) δ 159.36, 145.74, 144.65, 139.60, 139.29, 138.74, 135.79, 132.70, 132.35, 131.33, 130.51, 129.90, 128.94, 128.31, 127.59, 126.68, 126.41, 125.58, 125.11, 116.61, 115.27, 114.07, 70.56, 40.10, 32.38, 31.06, 30.15, 29.82, 29.59, 29.10, 23.51, 23.07, 13.97, 11.04, 10.44. MS (MALDI-Tof): Calcd. for $C_{62}H_{60}N_4O_3S_2$, 972.410; found, 971.581.

*2.3.6. Synthesis of 2-(6-((2-ethylhexyl)oxy)naphthalen-2-yl)-4,4,5,5-tetramethyl-1,3,2-dioxaborolane (**2b**)*

The synthetic procedure was similar to that of **2a**. Column chromatography over silica gel with petroleum ether/DCM (6/1) gives out target compound **2b** as colourless oil

liquid (4.9 g 52%). ^{1}H NMR (300 MHz, $CDCl_3$) δ 8.28 (s, 1H), 7.78 (t, J = 8.2 Hz, 2H), 7.70 (d, J = 8.2 Hz, 1H), 7.18 - 7.07 (m, 2H), 3.97 (d, J = 5.7 Hz, 2H), 1.87 - 1.72 (m, 1H), 1.57 (d, J = 6.2 Hz, 4H), 1.41 - 1.33 (m, 16H), 1.00 - 0.84 (m, 6H). ^{13}C NMR (101 MHz, $CDCl_3$) δ 158.40, 136.61, 136.07, 131.31, 131.11, 130.15, 128.35, 125.92, 119.15, 106.38, 83.78, 70.49, 39.43, 30.68, 29.18, 24.97, 24.02, 23.13, 14.18, 11.23. HRMS (EI+): [M+H$^+$] Calcd for $C_{24}H_{35}BO_3$, 383.2750; found, 383.2758.

*2.3.7. Synthesis of 3-bromo-10-(2-ethylhexyl)-7-(6-((2-ethylhexyl)oxy)naphthalen-2-yl)-10H-phenothiazine (**4b**)*

The synthetic procedure was similar to that of **4a**. Column chromatography over silica gel with petroleum ether/DCM (20/1) gives out target compound **4b** as light yellow oil liquid (5.1 g, 49%). ^{1}H NMR (400 MHz, $CDCl_3$) δ 7.87 (s, 1H), 7.74 (d, J = 8.6 Hz, 2H), 7.62 (dd, J = 8.5, 1.6 Hz, 1H), 7.47 (d, J = 7.9 Hz, 2H), 7.28 (d, J = 2.2 Hz, 1H), 7.23 (dd, J = 6.6, 2.0 Hz, 1H), 7.19 - 7.10 (m, 2H), 6.93 (d, J = 8.1 Hz, 1H), 6.71 (d, J = 8.6 Hz, 1H), 3.96 (d, J = 5.1 Hz 2H), 3.71 (s, 2H), 2.03-1.91 (m, 1H), 1.71-1.68 (m, 1H), 1.46 - 1.42 (m, 16H), 0.99 - 0.85 (m, 12H). ^{13}C NMR (101 MHz, $CDCl_3$) δ 157.54, 144.89, 144.43, 135.88, 134.87, 133.77, 129.90, 129.87, 129.53, 129.13, 127.79, 127.27, 126.11, 126.07, 125.51, 125.44, 124.85, 119.65, 117.01, 116.24, 114.49, 106.39, 70.61, 51.19, 39.45, 35.91, 30.75, 30.69, 29.20, 28.64, 24.05, 24.04, 23.16, 23.14, 14.20, 14.11, 11.25, 10.56. HRMS (EI+): [M+H$^+$] Calcd for $C_{38}H_{46}BrNOS$, 644.2566; found, 644.2555.

*2.3.8. Synthesis of 10-(2-ethylhexyl)-3-(6-((2-ethylhexyl)oxy)naphthalen-2-yl)-7-(4,4,5,5-tetramethyl-1,3,2-dioxaborolan-2-yl)-10H-phenothiazine (**6b**)*

The synthetic procedure was similar to that of **6a**. Column chromatography over silica gel with petroleum ether/DCM (4/1) gives out 2.8 g target compound **6b** as light yellow oil liquid. The yield is 51%. ^{1}H NMR (400 MHz, $CDCl_3$) δ 7.89 (s, 1H), 7.79 - 7.70 (m, 2H), 7.64 - 7.59 (m, 3H), 7.46 (d, J = 8.0 Hz, 2H), 7.15 (dd, J = 7.6, 5.2 Hz, 2H), 6.94 (d, J = 8.2 Hz, 1H), 6.88 (d, J = 8.1 Hz, 1H), 3.97 (d, J = 5.5 Hz, 2H), 3.78 (d, J = 5.3 Hz, 2H), 1.98 - 1.94 (m, 1H), 1.85 - 1.75 (m, 1H), 1.64 - 1.34 (m, 16H), 1.33 (s, 12H), 0.99 - 0.85 (m, 12H). ^{13}C NMR (101 MHz, $CDCl_3$) δ 157.47, 148.33, 144.33, 135.72,

135.02, 134.12, 133.70, 129.52, 129.12, 127.20, 126.29, 126.00, 125.74, 125.48, 124.79, 119.57, 116.21, 115.25, 106.37, 83.72, 70.59, 51.10, 39.43, 35.97, 30.77, 30.66, 29.76, 29.17, 28.65, 24.89, 24.05, 23.13, 14.17, 14.09, 11.22, 10.54. HRMS (EI+): [M+H^+] Calcd for $C_{44}H_{58}BNO_3S$, 692.4303; found, 692.4305.

*2.3.9. Synthesis of 3-(8-bromo-2,3-diphenylquinoxalin-5-yl)-10-(2-ethylhexyl)-7-(6-((2-ethylhexyl)oxy)naphthalen-2-yl)-10H-phenothiazine (**8b**)*

The synthetic procedure was similar to that of **8a**. Column chromatography over silica gel with petroleum ether/DCM (10/1) gives out 0.8 g target compound **8b** as red soild. The yield is 60%. ^{1}H NMR (400 MHz, CDCl3) δ 8.08 (d, J = 7.9 Hz, 1H), 7.91 (s, 1H), 7.76 (d, J = 8.6 Hz, 2H), 7.73 - 7.62 (m, 6H), 7.59 (dd, J = 7.8, 1.5 Hz, 2H), 7.55 - 7.46 (m, 2H), 7.43 - 7.26 (m, 6H), 7.20 - 7.12 (m, 2H), 7.01 (m, 2H), 3.97 (d, J = 5.5 Hz, 2H), 3.85 (s, 2H), 2.10 - 2.01 (m, 1H), 1.79 (dd, J = 12.2, 6.1 Hz, 1H), 1.53 - 1.31 (m, 16H), 0.98 - 0.87 (m, 12H). ^{13}C NMR (101 MHz, $CDCl_3$) δ 157.53, 154.09, 152.77, 152.40, 151.11, 145.50, 144.51, 139.34, 139.15, 138.91, 138.73, 138.62, 138.57, 138.03, 135.65, 135.03, 133.76, 133.13, 131.65, 130.36, 130.25, 129.97, 129.62, 129.38, 129.19, 128.42, 128.30, 127.30, 126.08, 125.93, 125.53, 124.87, 123.78, 122.70, 119.64, 116.27, 115.35, 106.46, 70.66, 39.51, 31.61, 30.92, 30.76, 30.39, 29.28, 28.81, 24.23, 24.11, 23.25, 14.33, 14.27, 11.36, 10.76. HRMS (EI+): [M+H^+] Calcd for $C_{58}H_{58}BrN_3OS$, 924.3557; found, 924.3561.

*2.3.10. Synthesis of the dye **ZHG6***

A mixture of compound **8b** (0.80 g, 0.86 mmol), **9** (0.27 g, 1.72 mmol), $Pd(PPh_3)_4$ (0.10 g, 0.09 mmol) and K_2CO_3 (0.36 g, 2.6 mmol) in 110 ml 1,4-dioxane/H_2O was heated at 100^{o}C overnight under N_2. The reaction solution was removed under vacuum and water was added. The water phase was then extracted with DCM. Combined organic phase was dried by Na_2SO_4. Column chromatography over silica gel with petroleum ether/DCM (2/1) gives out 0.62 g target compound **10b** as red solid and the yield is 75%. A mixture of compound **10b** (0.42 g, 0.44 mmol), cyanoacetic acid (0.75 g, 8.83 mmol) and NH_4OAc (1.02 g, 13.2 mmol) in 30 ml CH_3COOH solution was heated at 120^{o}C

overnight under N_2. The reaction solution was removed under vacuum and water was added. The water phase was then extracted with DCM. Combined organic phase was dried by Na_2SO_4. Column chromatography over silica gel with petroleum ether/DCM (1/1) gave out 0.21 g **ZHG6** dye as dark red solid and the yield is 47%. ^{1}H NMR (400 MHz, DMSO) δ 8.51 (d, J = 7.7 Hz, 1H), 8.12 (d, J = 17.5 Hz, 3H), 8.02 (d, J = 7.8 Hz, 1H), 7.98 - 7.71 (m, 8H), 7.63 (dd, J = 24.1, 7.4 Hz, 4H), 7.54 - 7.30 (m, 7H), 7.30 - 7.09 (m, 3H), 3.99 (d, J = 5.0 Hz, 2H), 3.91 (s, 2H), 1.94 (s, 1H), 1.76 (s, 1H), 1.50 - 1.24 (m, 16H), 1.00 - 0.72 (m, 12H). ^{13}C NMR (101 MHz, *D8*-THF) δ 157.49, 151.33, 145.20, 139.39, 138.03, 136.64, 135.41, 134.79, 133.95, 131.96, 130.23, 129.48, 129.40, 128.57, 127.89, 127.43, 127.26, 126.15, 125.58, 125.07, 124.62, 124.32, 119.17, 116.26, 115.08, 106.18, 70.13, 50.73, 39.59, 36.22, 31.34, 30.37, 29.71, 29.24, 28.62, 25.23, 24.19, 23.13, 23.05, 22.61, 13.52, 10.61, 10.00. MS (MALDI-Tof): Calcd. for $C_{66}H_{62}N_4O_3S_2$, 1022.426; found, 1022.661.

*2.3.11. Synthesis of 2-(2,2'-bis((2-ethylhexyl)oxy)-[1,1'-binaphthalen]-6-yl)-4,4,5,5-tetra-methyl-1,3,2-dioxaborolane (**2c**)*

The synthetic procedure was similar to that of **2a**, Column chromatography over silica gel with petroleum ether/DCM (6/1) gives out 7.3 g target compound **2c** as colourless oil liquid. The yield is 65%. ^{1}H NMR (300 MHz, $CDCl_3$) δ 8.38 (s, 1H), 7.94 (dd, J = 9.0, 9.0 Hz, 2H), 7.83 (d, J = 8.1 Hz, 1H), 7.54 (dd, J = 8.5, 1.0 Hz, 1H), 7.37 (dd, J = 8.9, 4.1 Hz, 2H), 7.31 - 7.26 (m, 1H), 7.21 - 7.09 (m, 3H), 3.86 - 3.68 (m, 4H), 1.36 (s, 12H), 1.33 - 1.21 (m, 6H), 0.95 - 0.85 (m, 12H), 0.76 – 0.64 (m, 6H), 0.62 - 0.50 (m, 6H). ^{13}C NMR (101 MHz, $CDCl_3$) δ 155.65, 154.67, 136.44, 136.07, 134.32, 130.55, 129.93, 129.16, 128.93, 128.51, 127.70, 125.94, 125.48, 124.61, 123.24, 120.51, 120.34, 115.51, 115.40, 114.99, 83.66, 71.90, 71.52, 71.38, 39.58, 39.49, 30.30, 28.96, 28.77, 24.89, 23.60, 23.48, 22.86, 14.02, 10.97. HRMS (EI+): [M+H$^+$] Calcd for $C_{42}H_{57}BO_4$, 637.4423; found, 637.4428.

*2.3.12. Synthesis of 3-(2,2'-bis((2-ethylhexyl)oxy)-[1,1'-binaphthalen]-6-yl)-7-bromo-10-(2-ethylhexyl)-10H-phenothiazine (**4c**)*

The synthetic procedure was similar to that of **4a**, column chromatography over

silica gel with petroleum ether/DCM (20/1) gives out 5.1 g target compound **4c** as light yellow oil liquid. The yield is 49%. ^{1}H NMR (300 MHz, $CDCl_3$) δ 8.00 - 7.89 (m, 3H), 7.85 (d, J = 8.2 Hz, 1H), 7.46 (d, J = 5.8 Hz, 2H), 7.39 (d, J = 9.0 Hz, 3H), 7.29-7.28 (m, 2H), 7.23 - 7.20 (m, 4H), 6.93 (d, J = 9.0 Hz, 1H), 6.73 (d, J = 8.8 Hz, 1H), 3.89 - 3.63 (m, 6H), 1.51 - 1.29 (m, 8H), 0.93-0.86 (m, 25H), 0.77 - 0.64 (m, 6H), 0.64 – 0.52 (m, 6H). ^{13}C NMR (101 MHz, $CDCl_3$) δ 154.82, 154.70, 154.67, 144.92, 144.34, 136.09, 134.56, 134.33, 133.47, 129.87, 129.42, 129.21, 129.05, 127.84, 127.78, 126.19, 126.11, 126.05, 125.52, 125.41, 125.13, 124.93, 123.31, 120.59, 120.51, 116.99, 116.19, 115.91, 115.87, 115.44, 114.44, 71.87, 71.70, 51.20, 39.55, 35.89, 30.74, 30.38, 30.31, 30.28, 29.77, 29.00, 28.84, 28.62, 24.04, 23.63, 23.52, 23.11, 22.93, 22.90, 22.89, 14.08, 11.04, 11.00, 10.96, 10.93, 10.54. HRMS (EI+): [M+H$^+$] Calcd for $C_{56}H_{68}BrNO_2S$, 898.4227; found, 898.4216.

*2.3.13.Synthesis of 3-(2,2'-bis((2-ethylhexyl)oxy)-[1,1'-binaphthalen]-6-yl)-10-(2-ethyl-hexyl)-7-(4,4,5,5-tetramethyl-1,3,2-dioxaborolan-2-yl)-10H-phenothiazine (**6c**)*

The synthetic procedure was similar to that of **6a**. Column chromatography over silica gel with petroleum ether/DCM (4/1) gives out 6.3 g target compound **6c** as light yellow oil liquid. The yield is 45%. ^{1}H NMR (400 MHz, $CDCl_3$) δ 7.99 - 7.88 (m, 3H), 7.84 (d, J = 8.1 Hz, 1H), 7.64 - 7.55 (m, 2H), 7.47 – 7.36 (m, 5H), 7.31 – 7.27 (m, 1H), 7.22 - 7.20 (m, 3H), 6.92 (d, J = 8.4 Hz, 1H), 6.87 (d, J = 8.0 Hz, 1H), 3.85 - 3.72 (m, 6H), 2.01 - 1.90 (m, 1H), 1.48 - 1.36 (m, 4H), 1.34 - 1.22 (m, 18H), 1.01 - 0.82 (m, 22H), 0.73 - 0.68 (m, 6H), 0.62 - 0.52 (m, 6H). ^{13}C NMR (101 MHz, $CDCl_3$) δ 154.75, 154.68, 148.35, 144.23, 135.91, 134.72, 134.32, 134.06, 133.41, 129.43, 129.19, 129.00, 127.73, 126.17, 126.11, 126.01, 125.72, 125.52, 125.17, 124.86, 124.76, 123.28, 120.54, 116.14, 115.88, 115.44, 115.21, 83.70, 71.87, 71.70, 51.08, 39.53, 35.93, 30.75, 30.35, 30.29, 30.26, 29.74, 28.98, 28.82, 28.63, 24.87, 24.04, 23.61, 23.50, 23.09, 22.90, 22.88, 14.06, 14.03, 11.01, 10.97, 10.93, 10.90, 10.52. HRMS (EI+): [M+H$^+$] Calcd for $C_{62}H_{80}BNO_4S$, 946.5974; found, 946.5981.

*2.3.14. Synthesis of 3-(8-bromo-2,3-diphenylquinoxalin-5-yl)-7-(4-((2-ethylhexyl)oxy)-phenyl)-10-octyl-10H-phenothiazine (**8c**)*

The synthetic procedure was similar to that of **8a**, column chromatography over silica gel with petroleum ether/DCM (9/1) gives out 0.8 g target compound **8c** as red soild. The yield is 60%.^{1}H NMR (400 MHz, $CDCl_3$) δ 8.08 (d, J = 7.8 Hz, 1H), 7.96 - 7.91 (m, 3H), 7.85 (d, J = 8.1 Hz, 1H), 7.74 - 7.61 (m, 5H), 7.59 (dd, J = 7.8, 1.5 Hz, 2H), 7.51 (s, 1H), 7.44 - 7.34 (m, 7H), 7.32 - 7.27 (m, 4H), 7.22 (s, 3H), 6.99 (br, 2H), 4.01 - 3.64 (m, 6H), 2.04 (s, 1H), 1.49 - 1.43 (m, 2H), 1.37 - 1.25 (m, 8H), 1.02 - 0.86 (m, 22H), 0.75 - 0.67 (m, 6H), 0.62 - 0.54 (m, 6H). ^{13}C NMR (101 MHz, $CDCl_3$) δ 154.83, 154.77, 152.79, 152.42, 145.56, 144.45, 139.16, 139.01, 138.74, 138.59, 138.54, 135.88, 134.95, 134.82, 134.41, 133.51, 133.09, 131.58, 130.30, 130.22, 129.91, 129.53, 129.43, 129.36, 129.28, 129.19, 129.10, 128.40, 128.28, 127.85, 126.21, 126.13, 125.93, 125.59, 125.29, 124.98, 123.38, 122.64, 120.66, 120.60, 116.20, 115.94, 115.49, 115.30, 71.92, 71.75, 51.17, 39.62, 36.06, 30.89, 30.46, 30.39, 30.35, 29.07, 28.91, 28.76, 24.19, 23.72, 23.60, 23.21, 23.01, 22.97, 14.19, 14.14, 11.13, 11.09, 11.04, 11.00, 10.69. HRMS (EI+): [M+H$^+$] Calcd for $C_{76}H_{80}BrN_3O_2S$, 1178.5227; found, 1178.5211.

*2.3.15. Synthesis of the dye **ZHG7***

A mixture of compound **8c** (2.75 g, 2.54 mmol), 9 (0.80 g, 5.08 mmol), $Pd(PPh_3)_4$ (0.30 g, 0.25 mmol) and K_2CO_3 (1.06 g, 7.62 mmol) in 110 ml 1,4-dioxane/H_2O was heated at 100^{o}C overnight under N_2. The reaction solution was removed under vacuum and water was added. The water phase was then extracted with DCM. Combined organic phase was dried by Na_2SO_4. Column chromatography over silica gel with petroleum ether/DCM (2/1) gives out 1.2 g target compound **10c** as red soild and the yield is 39%. A mixture of compound **10c** (0.21 g, 0.19 mmol), cyanoacetic acid (0.32 g, 3.78 mmol) and NH_4OAc (0.44 g, 5.67 mmol) in 30 ml CH_3COOH solution was heated at 120^{o}C overnight under N_2. The reaction solution was removed under vacuum and water was added. The water phase was then extracted with DCM. Combined organic phase was dried by Na_2SO_4. Column chromatography over silica gel with petroleum ether/DCM (1/1) gave out 0.089 g **ZHG7** dye as dark red solid and the yield is 21%. ^{1}H NMR (400

MHz, DMSO) δ 8.52 (d, J = 8.0 Hz, 1H), 8.22 (d, J = 8.0 Hz, 3H), 8.10 (dd, J = 9.1, 4.0 Hz, 2H), 8.03 (d, J = 9.1 Hz, 2H), 7.93 (d, J = 8.0 Hz, 1H), 7.89 – 7.67 (m, 5H), 7.67 – 7.51 (m, 6H), 7.50 - 7.07 (m, 10H), 7.02 (d, J = 8.4 Hz, 2H), 3.96 - 3.76 (m, 6H), 2.24 - 2.11 (m, 1H), 2.04 - 1.86 (m, 2H), 1.53 - 1.43 (m, 8H), 0.97 - 0.80 (m, 22H), 0.68 - 0.54 (m, 12H). ^{13}C NMR (101 MHz, *D8*-THF) δ 155.17, 151.67, 139.89, 138.86, 136.50, 134.79, 130.86, 130.13, 129.82, 129.49, 128.80, 128.03, 126.33, 126.14, 124.78, 123.41, 120.76, 119.66, 119.06, 116.62, 115.75, 71.62, 51.18, 40.14, 36.60, 33.86, 32.78, 30.44, 30.20, 30.50, 29.08, 29.03, 26.92, 24.75, 24.60, 24.40, 24.07, 23.93, 23.46, 23.27, 23.23, 23.04, 19.61, 13.94, 13.90, 10.96, 10.90, 10.89, 10.44. MS (MALDI-Tof): Calcd. for $C_{84}H_{84}N_4O_4S_2$, 1276.593; found, 1276.876.

3. Results and discussion

3.1. UV-Vis absorption properties

All the dyes are synthesized according to the routes shown in Scheme 1. In order to investigate their light-harvesting ability, we have carried out the test of UV absorption spectra of dyes in THF with 1 μM as shown in Fig. 2a. From the corresponding data collected in Table 1, we can see that the lowest energy absorption peak of **ZHG5**, **ZHG6** and **ZHG7** is 471 nm, 466 nm and 472 nm, respectively. These absorption bands around 466 - 472 nm can be ascribe to intramolecular charge transfer (ICT) from donor to acceptor along with π-π* transition [11]. The molar extinction coefficients of **ZHG5**, **ZHG6** and **ZHG7** are 1.98 × 10^4, 1.77 × 10^4 and 1.57 × 10^4 M^{-1} cm^{-1}, respectively. The UV absorption spectra of dyes in DCM and DMF are also carried out as shown in Fig. S1 and the corresponding data has been collected in Table S1. From the table, we can see that the kinds of solution have impacts on the absorption regions because the absorption bands are around 483-486 nm in DCM and 463-466 nm in DMF. The molar extinction coefficients also have been affected by the kinds of solution as shown in Table S1 and

they are 1.74×10^4, 1.61×10^4 and 1.31×10^4 M^{-1} $cm^{-1}$for three dyes in DCM, 1.95×10^4, 1.81×10^4 and 1.41×10^4 M^{-1} cm^{-1} for three dyes in DMF. Above results indicate that adjusting the auxiliary donor does not have significant influence on the absorption range of dyes but has impact on the absorption relative intensities. We also investigate the absorption properties of dyes anchored on the 12 μm thick nanocrystalline TiO_2 transparent film (particle size, 20 nm) as shown in Fig. 2b. From the data collected in the Table 1, it can note that compared with the maximum absorption peaks in the solution, there are 20 nm, 31nm and 27 nm red-shift for **ZHG5**, **ZHG6** and **ZHG7**, respectively. This red-shift could be ascribed to the J-aggregate and it facilitates the absorption range up to 700 nm which is thought to be helpful for light-harvesting [12].

3.2. Electrochemical properties

In order to investigate the feasibility of electron transfer from the excited dyes to the conduction band of TiO_2 and the dye regeneration by redox electrolyte, the cyclic voltammetry has been carried out in the THF solution as shown in Fig 3. From the parameters collected in the Table 1, we can see that the redox potentials correspond to the highest occupied molecular orbital (HOMO) energy levels of **ZHG5**, **ZHG6** and **ZHG7** are 1.28, 1.31 and 1.30 v *vs* NHE, respectively. These ground state oxidation potentials are all more positive than the redox potential of I^-/I_3^- (0.4 V *vs* NHE) which indicates that there are enough driving forces for the dyes regeneration as shown in Fig. S2. The band gap energies ($E_{0\text{-}0}$) of **ZHG5**, **ZHG6** and **ZHG7** derived from the absorption thresholds are 2.10, 2.16 and 2.12 V, respectively. Subtracting the $E_{0\text{-}0}$ from the E_{HOMO}, we can get the lowest unoccupied molecular orbital (LUMO) energy levels of **ZHG5**, **ZHG6** and

ZHG7 and they are -0.82, -0.85 and -0.82 V. All the LUMO levels are negative than that of the TiO_2 conduction band (-0.5 V vs. NHE), indicating enough power for the electron injection from the excited dyes to the TiO_2 conduction band. Therefore, all the three dyes could be the qualified candidates for DSSCs in theory [13].

3.3. Theoretical calculations

The electron distribution and molecular structures are investigated with density functional theory (DFT) calculations at the DFT B3LYP/LanL2DZ level with the Gaussian 09 suite of programs [14]. From the Fig. S3, we can see that the HOMO of **ZHG5** is mainly delocalized between auxiliary donor and quinoxaline. When the cyclobenzene is replaced by the naphthalene in **ZHG6**, the HOMO range has been further expanded. However, compared with **ZHG6**, the HOMO range of **ZHG7** is very similar with that of **ZHG6** when binaphthalene is adopted as auxiliary donor. The HOMO is just expand to one of the naphthalene rings and the other one does not have electron distribution which can be ascribe to the propeller type structure of binaphthalene. Although there is no electron distribution in the hanging naphthalene, it can effectively improve the steric hindrance. All LUMOs of these three sensitizers are delocalized between quinoxaline and the cyanoacrylic acid. The two benzene rings of 2,3-diphenylquinoxaline just have a little electron distribution which can be ascribe to the large torsion degree. These two non-coplanar cyclobenzenes can provide large steric effect and are beneficial for suppressing intermolecular dye aggregation. In general, the excellent overlap of HOMOs and LUMOs in three dyes will be helpful for the ICT from the donors to the acceptors [15].

3.4. Photovoltaic performance

All the DSSCs based on these three dyes have been tested under AM 1.5G irradiation (100 mW cm^{-2}) with I^-/I_3^- redox electrolyte and get their photocurrent density-voltage (*J-V*) curves as shown Fig. 4a. From the corresponding data collected in the Table 2, it can note that the modifying the auxiliary donors can produce obvious impact on the performance of DSSCs. DSSC based on the **ZHG5** has the highest power conversion efficiency (PCE) of 5.64% at AM 1.5 G simulated sunlight, with the short circuit current density J_{sc} = 12.63 mA cm^{-2}, open circuit voltage V_{oc} = 730 mV and *FF* = 0.61. When the cyclobenzene has been replaced by the naphthalene in the **ZHG6**, there is a little improvement of V_{oc} (734 mV), but the J_{sc} has decreased by 4.5%, only about 12.06 mA cm^{-2} and finally the PCE is decreased to 5.32%. The improvement of V_{oc} in the DSSC based on **ZHG6** encourages us to further increase the steric hindrance by introducing the dinaphthalene to get higher V_{oc}. To our surprise, the cell PCE further reduces to 2.74% with J_{sc} = 7.12 mA cm^{-2}, V_{oc} = 706 mV. In order to understand the order of J_{sc}, incident photon-to-current conversion efficiencies (IPCE) have been carried out. From the Fig. 4b, it can note that the IPCE of all the DSSCs based on these three dyes have the similar absorption range from 300 nm to 700 nm. Compared with the **ZHG6**, the IPCE value of **ZHG5** is a little higher than that of **ZHG6** from the 400 nm to 550 nm and both of them are much higher than the IPCE of **ZHG7** over the whole absorption range. So the J_{sc} values of DSSCs based on these dyes increase in the order of **ZHG5** > **ZHG6** > **ZHG7.**

Electrochemical impedance measurements under the dark with -0.7 V bias have been carried out to investigate the electron recombination effect of the cell devices and get insight to the open circuit voltage [16]. In general, the larger semicircle of the Nyquist

plot in the high frequency region represents the charge recombination resistance (R_{rec}) at the photoanode/dye/electrolyte interface. The smaller semicircle corresponds to electron transport at the Pt/electrolyte. From the Fig. 5a, it can note that the R_{rec} value of DSSC based on dye **ZHG6** is higher than that of **ZHG5**, and the R_{rec} of **ZHG7** is the smallest. So the R_{rec} increases in the order of **ZHG6** > **ZHG5** >**ZHG7**. This order is the same as the open circuit voltage. The lifetimes have been calculated with the formula $\tau = 1/(2\pi f)$ from the Bode plots as shown in Fig. 5b. Because the *f* values of **ZHG5**，**ZHG6** and **ZHG7** from the Bode plots are 2.69 Hz, 2.37 Hz and 2.86 Hz, respectively. So the lifetimes of **ZHG5**, **ZHG6** and **ZHG7** are 59.19 ms, 67.19 ms and 55.67 ms, respectively. Longer lifetimes correspond to lower current in the dark of DSSCs and the order of lifetimes is also consist with that of V_{oc} [17].

4. Surface adsorption properties

In order to investigate the different performances caused by tuning the auxiliary donors, the XPS has been used to investigate the adsorption properties of dyes anchored on the TiO_2 surface [18]. The sensitizers loading amount of all DSSCs have been investigated by the dye desorption measurements before the XPS test. From the collected data in the Table 3, it can note that the adsorption capacities of **ZHG5**, **ZHG6** and **ZHG7** are 7.6×10^{-6}, 5.6×10^{-6} and 8.3×10^{-6} mol cm^{-2}. When the value of **ZHG5** is set to 1, the relative value of **ZHG6** and **ZHG7** is 0.74 and 1.09. The relative loading amounts of ZHG dyes anchored on TiO_2 also have been measured with XPS by comparing the intensity of the S2p core level and the $Ti2p_{3/2}$ level as shown in Fig. 6a. From the data summarized in the Table 3, we can

see that when the value of **ZHG5** is set to 1, the relative value of **ZHG6** and **ZHG7** is 0.9 and 2.0. The relative values measured by the above two methods are consistent and indicate that the dyes loading amount increases in the order of **ZHG7** > **ZHG5** >**ZHG6**. In order to understand this phenomenon, we have carefully compared the $Ti2p_{3/2}$ intensity (*I*) damping of the TiO_2 film anchored by the corresponding sensitizers with the intensity (I_0) damping of blank TiO_2 film as summarized in Table S1 (ESI†) and got the mean thickness (*d*) of dye coverage. From Fig. 6b, it can note that the $Ti2p_{3/2}$ intensity of TiO_2 covered by sensitizers is apparent lower than that of blank TiO_2 sample, especially for the dye with dinaphthalene. If the dye layers are homogeneous and all TiO_2 samples only have small amount of contaminants, the mean thickness (*d*) can be calculated by a two-layer model $I/I_0 = \exp(-d/\lambda\sin\alpha)$ where λ is the inelastic mean free path (IMFP) of electrons in dye molecules, α is the electron take-off angle of 45^o. The IMFP of **ZHG5**, **ZHG6** and **ZHG7** is 25.95 Å, 30.25 Å and 30.37 Å, respectively [19]. So we can get the mean thickness of dye coverage for **ZHG5**, **ZHG6** and **ZHG7**, their values are 12.81 Å, 13.44 Å and 27.24 Å, respectively [20]. Considering the molecular size we can conclude that the **ZHG7** dye on the TiO_2 film is almost standing rather vertical on the TiO_2 film with the smallest tilt angles and the tilt angles of **ZHG5** and **ZHG6** are almost similar. Because the anchored modes of **ZHG5** and **ZHG6** on the TiO_2 are similar, the lower dye loading amount of **ZHG6** can be ascribe to larger steric hindrance of auxiliary donor. The lower IPCE value of **ZHG6** compared with that of **ZHG5** from the 400 nm to 500 nm can be ascribe to the lower molar extinction coefficient and dye loading amount and finally leads to

lower J_{sc}. Although the **ZHG7** has auxiliary donor with the maximal steric hindrance, it still has the highest dye loading amount probably due to the smallest tilt angle. This is in accord with the result found by Anders Hagfeldt et al.,[21] where the larger tilt angle found for the LEG4 dye with respect to the TiO_2-surface normal compared to the other dyes is likely to result in less efficient packing of the dye molecules. Dense packing of dye **ZHG7** anchored on the TiO_2 leads to more serious intermolecular π-π aggregation effect and we also carry out the test of cell performance based on **ZHG7** with chenodeoxycholic acid (CDCA). From the data collected in Table 2 and Fig. S4, we can see that PCE is improved to 3.37% with J_{sc} = 9.17 mA cm^{-2}, V_{oc} = 693mV. So the addition of co-adsorbent is good for improving the cell performance of **ZHG7** dye. So perhaps the π-π aggregation effect and lowest molar extinction coefficient are the reasons that DSSC based on **ZHG7** has the poor performance.

5. Conclusion

Three novel D-D-π-A Sensitizers **ZHG5**, **ZHG6** and **ZHG7** have been prepared by gradually improving the steric hindrance of auxiliary donors. The DSSCs based on these three dyes have been carefully investigated by the electrochemical, photophysical, photovoltaic characterizations and XPS in combination with theoretical calculations. XPS indicates that the tilt angles of **ZHG5** and **ZHG6** anchored on the TiO_2 film are similar and **ZHG7** is almost standing rather vertical on the TiO_2 film with the smallest tilt angle. Dye desorption experiment and XPS indicate that the dye loading amount of **ZHG6** is lower than **ZHG5** due to the larger steric hindrance and **ZHG7** with largest

auxiliary donor has the maximum loading amount probably due to the smallest tilt angle. Larger auxiliary donor of **ZHG6** can lead to higher open circuit voltage but lower shorter circuit current (J_{sc} = 12.63 mA cm^{-2}) compared with that of **ZHG5**. However, dense packing of dye **ZHG7** anchored on the TiO_2 leads to more serious intermolecular π-π aggregation effects and perhaps this effect and lowest molar molecular extinction coefficient are the reason that DSSC based on **ZHG7** have the poor performance. So above results indicate that auxiliary donor with overlarge steric hindrance will have smaller tilt angle of dye anchored on TiO_2 and may lead to more dye loading amount but serious intermolecular π-π aggregation effects. We think that this result can provide some enlightenment for the future research of the structure-activity relationship of dyes.

Acknowledgements

We would like to kindly acknowledge the National Natural Science Foundation of China (No. 21371092), and National Basic Research Program of China (2010CB923303).

References

[1] (a) O'Regan B, Grätzel M. A low-cost high-efficiency solar cell based on dye-sensitized colloidal TiO_2 films. Nature 1991; 353: 737-740. (b) Xie YS, Tang YY, Wu WJ, Wang YQ, Liu JC, Li X, Tian H, Zhu WH. Porphyrin Cosensitization for a Photovoltaic Efficiency of 11.5%: A Record for Non-Ruthenium Solar Cells Based on Iodine Electrolyte. J. Am. Chem. Soc. 2015; 13: 14055-14058. (c) Xie YS, Wu WJ, Zhu HB, Liu JS, Zhang WW, Tian H, Zhu WH. Unprecedentedly targeted customization of molecular energy levels with auxiliary-groups in organic solar cell

sensitizers. Chem. Sci. 2016; 7: 544-49. (d) Tang J, Wu WJ, Hua JL, Li J, Li X, Tian H. Starburst triphenylamine-based cyanine dye for efficient quasi-solid-state dye-sensitized solar cells. Energy Environ. Sci. 2009; 2: 982–990.

[2] (a) Nazeeruddin M, Kay A, Rodicio I, HumpbryBaker R, Miiller E, Liska P, Vlachopoulos N, Grätzel M, Conversion of Light to Electricity by cis-X_2Bis(2,2´-bipyridyl-4,4´-dicarboxylate)ruthenium(Ⅱ) Charge Transfer Sensitizers (X = C1-, Br-, I-, CN-, and SCN-) on Nanocrystalline TiO_2 Electrodes. J. Am. Chem. Soc 1993; 115: 6382-6390. (b) Mathew S, Yella A, Gao P, Humphry-Baker R, Curchod B, Ashari-Astani N, Tavernelli I, Rothlisberger U, Nazeeruddin M, Grätzel M, Dye-sensitized solar cells with 13% efficiency achieved through the molecular engineering of porphyrin sensitizers Nat. Chem. 2014; 6: 242-247.

[3] (a) Wu YZ, Zhu WH, Zakeeruddin S, Grätzel M. Insight into D−A−π−A Structured Sensitizers: A Promising Route to Highly Efficient and Stable Dye-Sensitized Solar Cells. ACS Appl. Mater. Interfaces 2015; 7: 9307-9318.（b）Jradi F, Kang XW, O'Neil D, Pajares G, Getmanenko Y, Szymanski P, Parker T, El-Sayed M, Marder S. Near-Infrared Asymmetrical Squaraine Sensitizers for Highly Efficient Dye Sensitized Solar Cells: The Effect of π-Bridges and Anchoring Groups on Solar Cell Performance. Chem. Mater. 2015; 27: 2480-2487. (c) Hu Y, Ivaturi A, Planells M, Boldrini C, Birolib A, Robertson N. 'Donor-free' oligo(3-hexylthiophene) dyes for efficient dye-sensitized solar cells. J. Mater. Chem. A 2016; 4: 2509-2516.

[4] Kakiage K, Aoyama Y, Yano T, Oya K, Fujisawab J, Hanaya M. Highly-efficient dye-sensitized solar cells with collaborative sensitization by silyl-anchor and

carboxy-anchor dyes. Chem. Commun. 2015; 51: 15894-15897.

[5] Feldt S, Gibson E, Gabrielsson E, Sun LC, Boschloo G, Hagfeldt A. Design of Organic Dyes and Cobalt Polypyridine Redox Mediators for High-Efficiency Dye-Sensitized Solar Cells. J. Am. Chem. Soc. 2010; 132: 16714-16724.

[6] Zhang XY, Mao JY, Wang D, Li X, Yang JB, Shen ZJ, Wu WJ, Li J, Ågren H, Hua JL. Comparative Study on Pyrido[3,4-b]pyrazine-Based Sensitizers by Tuning Bulky Donors for Dye-Sensitized Solar Cells. ACS Appl. Mater. Interfaces 2015; 7: 2760-2771.

[7] Wu SH, Yang L, Li Y, Zhang M, Zhang J, Guo YC, Wang P. Unlocking the effects of ancillary electron-donors on light absorption and charge recombination in phenanthrocarbazole dye-sensitized solar cells. J. Mater. Chem. A 2016; 4: 519-528.

[8] Li SR, Lee CP, Kuo HT, Ho KC, Sun SS. High-Performance Dipolar Organic Dyes with an Electron-Deficient Diphenylquinoxaline Moiety in the p-Conjugation Framework for Dye-Sensitized Solar Cells. Chem. Eur. J. 2012; 18: 12085-12095.

[9] Song JL, Amaladass P, Wen SH, Pasunooti KK, Li A, Yu YL, Wang X, Deng WQ, Liu XW. Aryl/hetero-arylethyne bridged dyes: the effect of planar p-bridge on the performance of dye-sensitized solar cells. New J. Chem. 2011; 35: 127-136.

[10] (a) Shen ZJ, Chen J, Li X, Li X, Zhou Y, Yu Y, Ding HR, Li J, Zhu LY, Hua JL. Synthesis and Photovoltaic Properties of Powerful Electron-Donating Indeno[1, 2-b]thiophene-Based Green D-A-π-A Sensitizers for Dye Sensitized Solar Cells. ACS Sustainable Chem. Eng. 2016: 4: 3518-3525. (b) Cheng JX, Huang ZS, Wang LY, Cao DR. D-π-A-π-A featured dyes containing different electronwithdrawing auxiliary acceptors: The impact on photovoltaic performances. Dyes and Pigments

2016; 131: 134-144.

[11] Hua Y, He J, Zhang CS, Qin CJ, Han LY, Zhao JZ, Chen T, Wong WY, Wong WK, Zhu XJ. Effects of various p-conjugated spacers in thiadiazole[3,4-c]pyridine-cored panchromatic organic dyes for dye-sensitized solar cells. J. Mater. Chem. A 2015; 3: 3103-3112.

[12] Li SL, Jiang KJ, Shao KF, Yang LM. Novel organic dyes for efficient dye-sensitized solar cells. Chem. Commun., 2006; 26: 2792-2794.

[13] Li HY, Fang MM, Tang RL, Hou YQ, Liao QY, Mei AY, Han HW, Li QQ, Li Z. The introduction of conjugated isolation groups into the common acceptor cyanoacrylic acid: an efficient strategy to suppress the charge recombination in dye sensitized solar cells and the dramatically improved efficiency from 5.89% to 9.44%. J. Mater. Chem. A, 2016; 4: 16403-16409.

[14] Gao YT, Li X, Hu Y, Fan YL, Yuan JY, Robertson N, Hua JL, Marder SR. Effect of an auxiliary acceptor on D-A-π-A sensitizers for highly efficient and stable dyesensitized solar cells. J. Mater. Chem. A, 2016; 4: 12865-12877.

[15] Li CM, Luo L, Wu D, Jiang R, Lan JB, Wang RL, Huang LY, Yang SY, You JS. Porphyrins with intense absorptivity: highly efficient sensitizers with a photovoltaic efficiency of up to 10.7% without a cosensitizer and a coabsorbate. J. Mater. Chem. A, 2016; 4: 11829-11834.

[16] Soni S, Fadadu K, Vaghasiya J, Solanki B, Sonigara K, Singh A, Das D, Iyer P. Improved molecular architecture of D-π-A carbazole dyes: 9% PCE with a cobalt redox shuttle in dye sensitized solar cells. J. Mater. Chem. A 2015; 3: 21664-21671.

[17] Jia HL, Ju XH, Zhang MD, Ju ZM, Zheng HG. Effects of heterocycles containing

different atoms as p-bridges on the performance of dye-sensitized solar cells. Phys. Chem. Chem. Phys. 2015; 17: 16334-16340.

[18] Hahlin M, Johansson E, Plogmaker S, Odelius M, Hagberg D, Sun LC, Siegbahna H, Rensmo H. Electronic and molecular structures of organic dye/TiO_2 interfaces for solar cell applications: a core level photoelectron spectroscopy study. Phys. Chem. Chem. Phys. 2010; 12: 1507-1517.

[19] Cao YM, Cai N, Wang YL, Li RZ, Yuan Y, Wang P. Modulating the assembly of organic dye molecules on titania nanocrystals via alkyl chain elongation for efficient mesoscopic cobalt solar cells. Phys. Chem. Chem. Phys., 2012; 14: 8282-8286.

[20] Cumpson P. Estimation of inelastic mean free paths for polymers and other organic materials: use of quantitative structure–property relationships. Surf. Interface Anal. 2001; 31: 23-34.

[21] Hanna E, Susanna K. E, Sandra M. F, Erik G, Peter W. L, Rebecka L, Sun LC, Hakan R, Gerrit B, Anders H. Linker Unit Modification of Triphenylamine-Based Organic Dyes for Efficient Cobalt Mediated Dye-Sensitized Solar Cells. J. Phys. Chem. C 2013; 117; 21029-21036.

Table 1 Absorption and electrochemical paramaters of dyes

Dye	λ_{max}[a]/nm ($\varepsilon\times10^4 M^{-1}$ cm^{-1})	λ_{max}[b]/nm	E_{ox}[c]/V (vs. NHE)	$E_{0\text{-}0}$[d]/eV	E_{red}[e]/V (vs. NHE)
ZHG5	471 (1.98)	491	1.28	2.10	-0.82
ZHG6	466 (1.77)	497	1.31	2.16	-0.85
ZHG7	472 (1.57)	499	1.30	2.12	-0.82

[a] Absorption maximum in 1×10^{-6} M THF solution. [b] Absorption maximum on TiO_2 film. [c] Oxidation potential in THF solution containing 0.1 M $(n\text{-}C_4H_9)_4NPF_6$ were calibrated with (Fc/Fc^+) as an external reference and taken as the HOMO. [d] $E_{0\text{-}0}$ derived from the oneset of UV-Vis absorption spectrum. [e] $E_{red} = E_{ox} - E_{0\text{–}0}$.

Table 2 Photovoltaic parameters of the DSSCs obtained from the J–V curves

Dye[a]	J_{sc} (mA cm^{-2})	V_{oc} (mV)	FF (%)	η (%)
ZHG5	12.63±0.39	730±2	61.75±0.27	5.64±0.23
ZHG6	12.06±0.12	734±4	60.06±0.88	5.32±0.10
ZHG7	7.12±0.17	706±2	54.63±0.22	2.74±0.08
ZHG7*	9.17±0.24	693±5	53.07±0.78	3.37±0.02

[a] The DSSCs are measured under AM 1.5G irradiation, the photoanode was immersed in THF/EtOH solution of the ZHG dyes (0.3 mM) for 12 h.* the photoanode was immersed in THF/EtOH solution of the 0.3 mM ZHG7+0.5mM CDCA for 12 h.

Table 3 Dye Coverage of the TiO_2-Surface, Measured both by Dye Desorption Measurements and by XPS

Dye coverage/ mol cm^{-2} (dye desorption)	Relative dye coverage (dye desorption)	Relative dye coverage (XPS)
7.6×10^{-6}	1	1
5.6×10^{-6}	0.74	0.90
8.3×10^{-6}	1.09	2.00

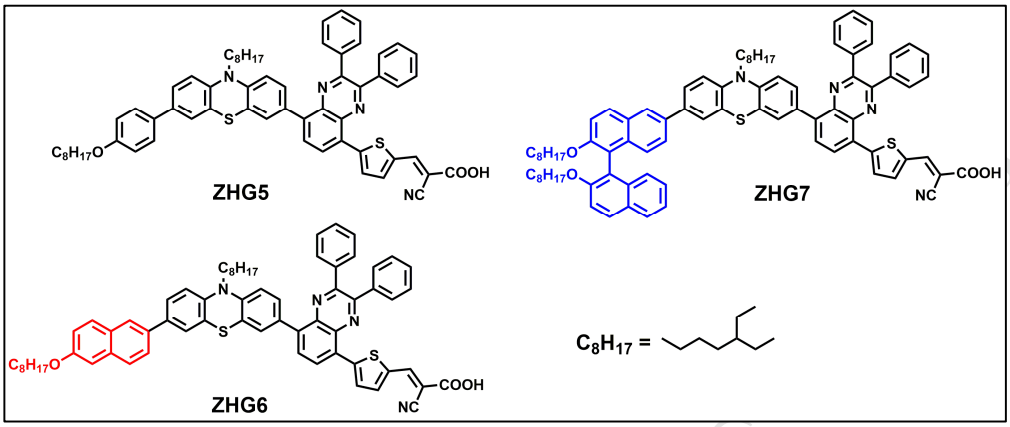

Fig. 1 Chemical structures of **ZHG5**, **ZHG6** and **ZHG7.**

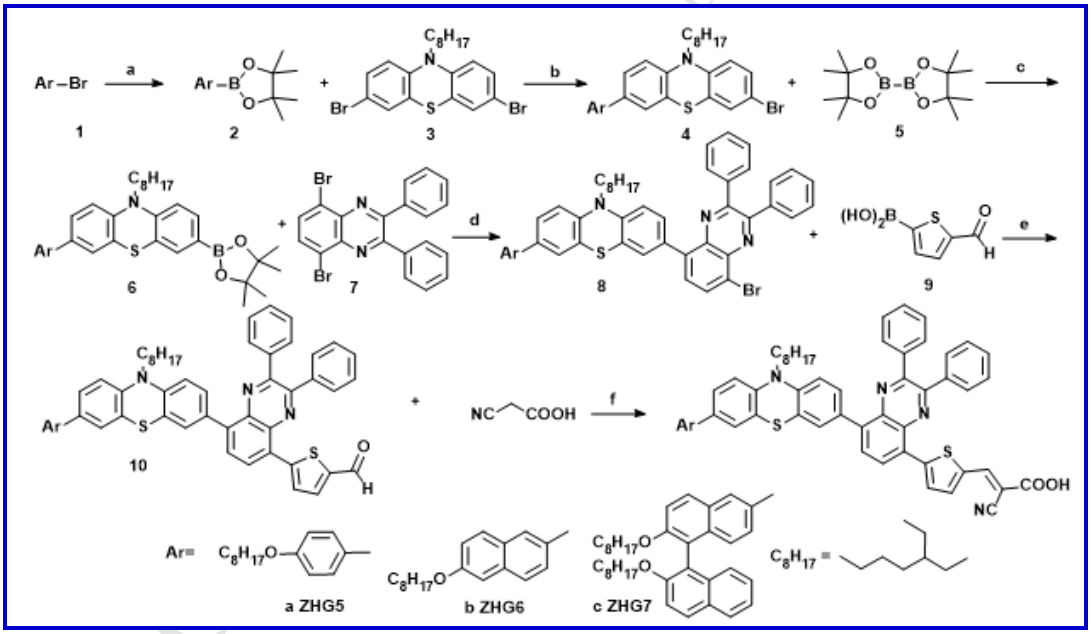

Scheme 1 Reagents and conditions: (a) $Pd(PPh_3)_4$, Bis(pinacolato)diboron, KOAc, 1,4-Dioxane, 100 ^oC; (b) $Pd(PPh_3)_4$, K_2CO_3, 1,4-Dioxane/H_2O, 100 ^oC; (c) $Pd(PPh_3)_4$, KOAc, 1,4-Dioxane, 100 ^oC; (d) $Pd(PPh_3)_4$, K_2CO_3, 1,4-Dioxane/H_2O, 100 ^oC; (e) $Pd(PPh_3)_4$, K_2CO_3, 1,4-Dioxane/H_2O, 100 ^oC; (f) AcOH, NH_4OAc,120 ^oC.

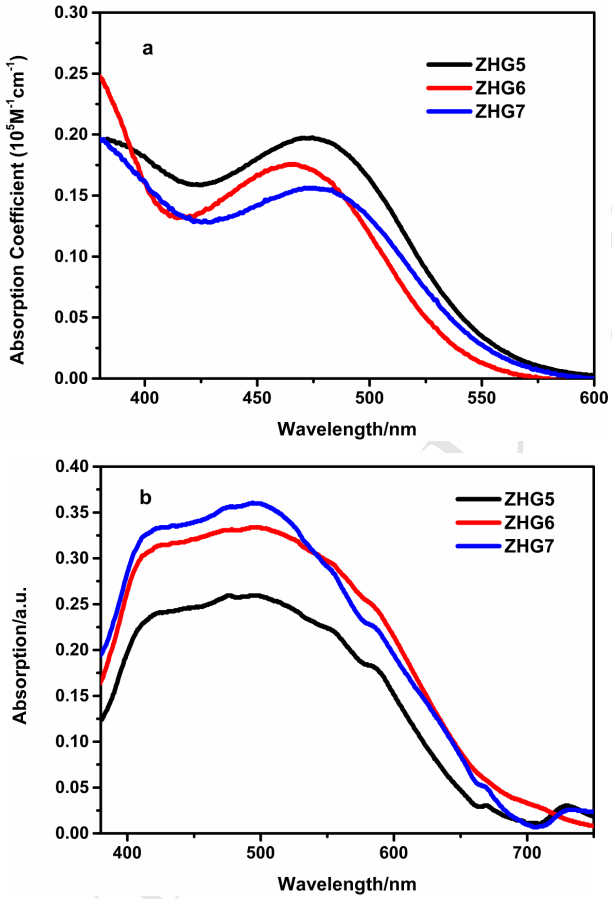

Fig. 2 (a) UV-Vis absorption spectra of dyes in THF solution. (b) UV-Vis absorption spectra of dyes on TiO_2 films.

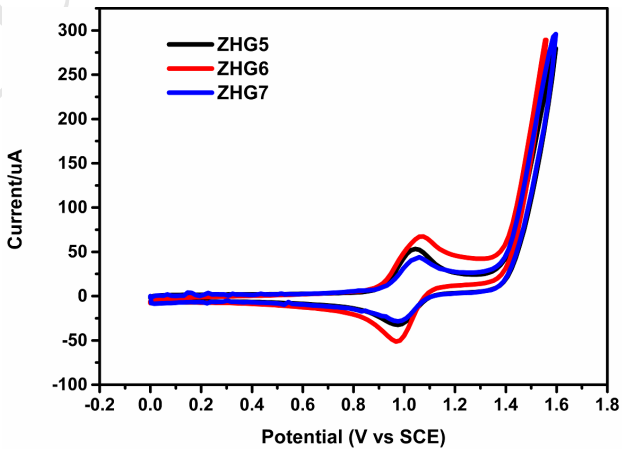

Fig. 3 Cyclic voltammograms of dyes in THF. (0.1 M $TBAPF_6$, glassy carbon electrode as working electrode, Pt as counter electrode, SCE as reference electrode, scan rate: 100 mV s^{-1})

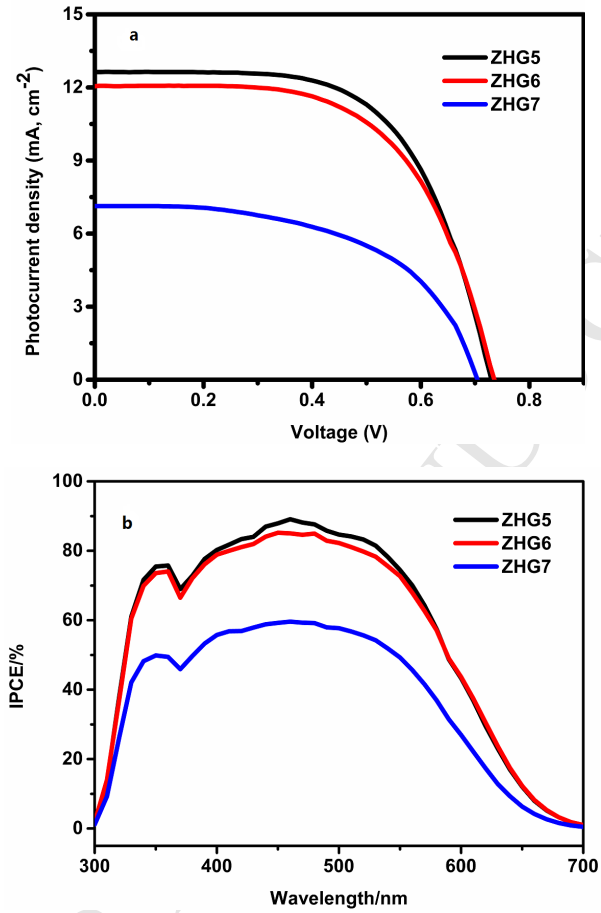

Fig. 4 (a) The J–V curves of DSSCs based on ZHG dyes. (b) The IPCE curves of DSSCs based on ZHG dyes.

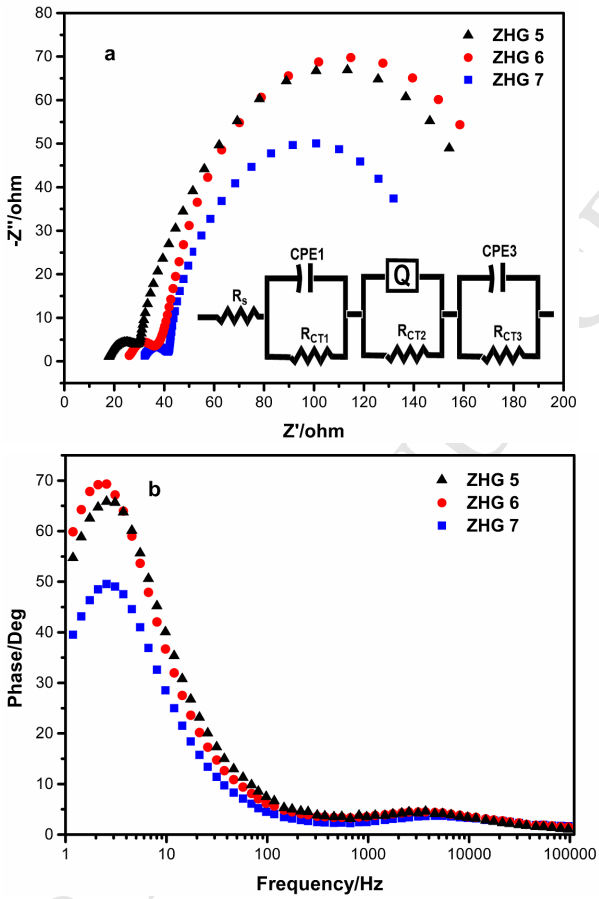

Fig. 5 (a) Nyquist plots of DSSCs based on ZHG dyes, the equivalent circuit used in the study. (b) Bode phase plots obtained in the dark under bias (-0.7 V) for DSSCs based on ZHG dyes.

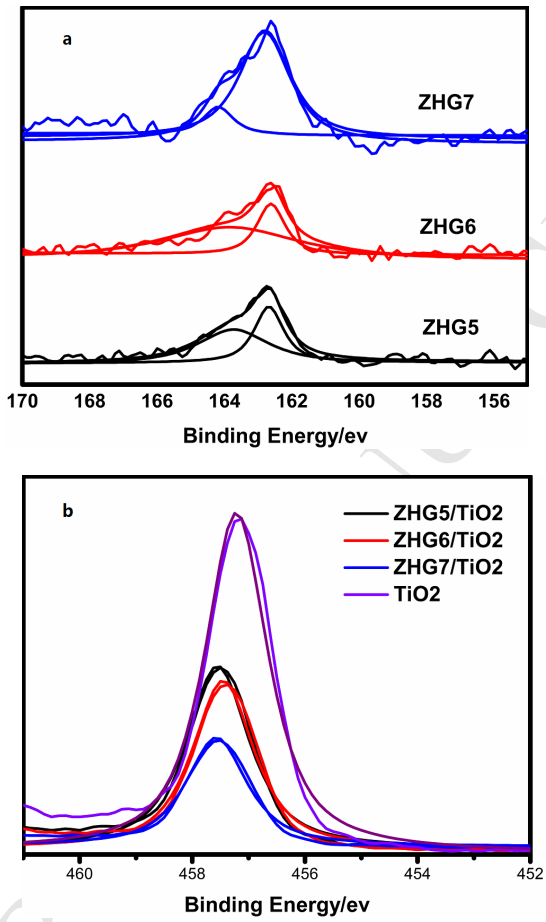

Fig. 6 (a) The S2p spectra normalized versus the corresponding Ti2p and (b) The $Ti2p_{3/2}$ photoelectron signal originating from the TiO_2.

Fig. 1 Chemical structures of **ZHG5**, **ZHG6** and **ZHG7**.

Fig. 2 (a) UV-Vis absorption spectra of dyes in THF solution. (b) UV-Vis absorption spectra of dyes on TiO_2 films.

Fig. 3 Cyclic voltammograms of dyes in THF. (0.1 M $TBAPF_6$, glassy carbon electrode as working electrode, Pt as counter electrode, SCE as reference electrode, scan rate: 100 mV s^{-1})

Fig. 4 (a) The J–V curves of DSSCs based on ZHG dyes. (b) The IPCE curves of DSSCs based on ZHG dyes.

Fig. 5 (a) Nyquist plots of DSSCs based on ZHG dyes, the equivalent circuit used in the study. (b) Bode phase plots obtained in the dark under bias (-0.7 V) for DSSCs based on ZHG dyes.

Fig. 6 (a) The S2p spectra normalized versus the corresponding Ti2p and (b) The $Ti2p_{3/2}$ photoelectron signal originating from the TiO_2.

- Three novel dyes are prepared by tuning the steric hindrance of auxiliary donors.
- Adsorption properties of dyes are studied with X-ray photoelectron spectroscopy.
- Dye with largest auxiliary donor has the smallest tilt angle on TiO_2.